A self-assembly SHS approach to form silicon carbide nanofibres

2007 J. Phys.: Condens. Matter 19 395022

(http://iopscience.iop.org/0953-8984/19/39/395022)

IOP PUBLISHING JOURNAL OF PHYSICS: CONDENSED MATTER

J. Phys.: Condens. Matter **19** (2007) 395022 (10pp) doi:10.1088/0953-8984/19/39/395022

A self-assembly SHS approach to form silicon carbide nanofibres

A Huczko[1], M Osica[1], A Rutkowska[1], M Bystrzejewski[1], H Lange[1] and S Cudziło[2]

[1] Department of Chemistry, Warsaw University, 1 Pasteur street, 02-093 Warsaw, Poland
[2] Institute of Chemistry, Military University of Technology, 2 Kaliski street, 00-908 Warsaw, Poland

E-mail: ahuczko@chem.uw.edu.pl

Received 16 February 2007, in final form 24 April 2007
Published 30 August 2007
Online at stacks.iop.org/JPhysCM/19/395022

Abstract

β-SiC nanofibres were efficiently produced using the thermal-explosion mode of self-propagating high-temperature synthesis from elemental Si and poly(tetrafluoroethylene) powder mixtures combusted under different operational parameters. The averaged combustion temperatures were evaluated using emission spectroscopy to be above 2000 K. The solid products were characterized by scanning and transmission electron microscopy, chemical analysis, and x-ray diffraction. Under optimum conditions the conversion of starting elemental Si into products exceeded 90%. To obtain pure (about 90%) SiC nanofibres the solid products were processed by wet chemistry.

1. Introduction

Self-propagating high-temperature synthesis (SHS) is a combustion process that results in the formation of valuable condensed products for practical purposes [1–3]. The uniqueness and advantages of the SHS process and its adaptability in the processing of materials provide a way for the formation of novel compounds and structures that are otherwise difficult to produce under conventional conditions. Combustion synthesis has a specific characteristic, i.e., the initial solid substrates react in a self-propagating regime with high self-heating and can form a host of hard refractory products: oxides, borides, carbides, nitrides, silicides, and cermets [4–6] at high combustion temperature. The process begins with an activation period that is followed by a strong exothermic reaction that propagates rapidly through the solid reactants [7] and is usually completed within a fraction of a second [8–10]. Rapid solidification or condensation of reaction products may create nanostructures that would be unstable under normal conditions, e.g., fast cooling can lead to the nucleation of nanocrystallites [11, 12]. It is worth noticing here that Howard *et al* [13] developed the synthesis of fullerenes at MIT via a combustion synthesis route.

Recently [14, 15] we reported the formation of one-dimensional (1D) Si-containing nanometric structures through the de-fluorination of poly(tetrafluoroethylene) (PTFE) using an SHS route. Specific carbon-based nanostructures, e.g., encapsulates, onions and carbides, were also spontaneously formed [16] by an SHS-induced carbonization of halocarbons according to the following complex scheme:

$$(1+m)\mathrm{CX}_n + (n+m)\mathrm{Me} \rightarrow n\mathrm{MeX} + m\mathrm{MeC} + \mathrm{C} + nm/2\mathrm{X}_2.$$

Silicon carbide exhibits a set of unique physical parameters, which makes it a promising candidate for electronic (MEMS), composites and other high-temperature and harsh-environment applications. 1D SiC nanostructures have new properties resulting from both marked shape-specific and quantum-confinement effects. Previously we reported the application of SHS-produced SiC nanofibres as a resonant mass sensor [17]. We also evaluated the optical limiting performance of these nanofibres [18].

All methods of preparing 1D SiC nanostructures are quite involved [19–21]. Previous combustion synthesis via $CaSi_2$/PTFE mixtures efficiently yielded [14, 15] β-SiC nanofibres. However, the solid product was contaminated with CaF_2, thus making the purification procedure much more labour intensive. In this paper we present the results of a parametric study on the spontaneous formation of silicon carbide nanofibres by reductive de-fluorination of PTFE with elemental Si.

2. Experiment

The SHS experiments were conducted in a modified calorimetric bomb [14–16] on powder mixtures of elemental Si and PTFE to study the effect of operational parameters on solid-state chemical synthesis. The starting two-component mixtures were prepared from irregularly shaped Si (Alfa Aesar, 99%) and PTFE (Aldrich, 99%) micro-powders in an equiatomic stoichiometry Si(36%)/PTFE(64%), tumbled in a mechanical shaker for 15 min. The composition of the starting reactants resulted from the reaction scheme represented by

$$2\mathrm{Si} + 2\mathrm{CF}_2 \rightarrow \mathrm{SiC} + \mathrm{SiF}_4 + \mathrm{C}$$

which exploratory testing had proved earlier [14] to be the most favourable for SiC formation. The process protocol comprises the steps of (i) placing a powdery mixture in a quartz crucible inside a calorimetric bomb, (ii) igniting the SHS mixture using ohmic heating so that the redox reaction takes place and the reducible PTFE is reduced to elemental carbon while the strongly reductive elemental Si is partially oxidized to the fluoride and carbide. To study the influence of environmental conditions, the bomb was initially filled with various gases at different initial pressure, or else the grain size of the starting charge was changed. The combustion is accompanied by the abrupt evolution of heat resulting from the high temperature, and a pressure increase in the system, which was monitored. After the combustion was completed, the gaseous products were vented and the products, soot-like or very voluminous, sponge-like grey solids, were collected for further analyses.

The calorimetric bomb was equipped with an observation port to detect the light emitted from the combustion zone. The light emission was recorded by VSMS™ broadband, high-resolution spectrograph (Acton Research Corp.). The spectrum was radiometrically corrected by using an NBS 1000 W quartz iodine lamp. Since a continuum spectrum was the main feature of the emission spectrum, it served for the gas temperature determination by using Planck's equation for black body radiation:

$$F(\lambda) = \frac{hc}{\lambda^5}\left(\exp\left(\frac{hc}{k}\frac{1}{\lambda T}\right) - 1\right)^{-1}$$

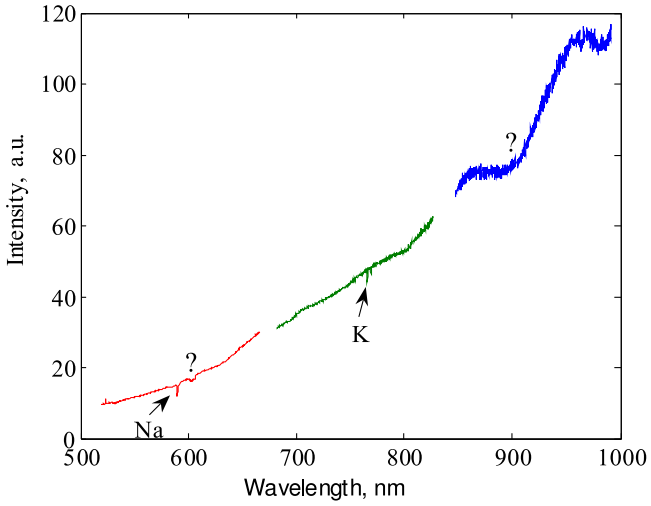

Figure 1. Emission spectrum of radiation emitted from the combustion zone.
(This figure is in colour only in the electronic version)

where $F(\lambda)$ is the spectral emissive power, h is Planck's constant, c is the speed of light, k is the Boltzmann constant, λ is the wavelength, and T is the temperature.

The microstructural and chemical characterization of products was performed using x-ray diffraction (XRD; Siemens diffractometer D 500, Cu Kα radiation), scanning electron microscopy (SEM; LeO 500) and transmission electron microscopy (TEM; FEI Tecnai F30), and elemental analysis (Perkin–Elmer analyser CHNS/0, model 2400). The amount of unreacted elemental Si in the product was estimated by dissolving the sample in boiling KOH_{aq} and measurement of the volume of evolved hydrogen.

3. Results and discussion

The emission spectrum recorded in a wide spectral range (500–1000 nm) during combustion synthesis under argon atmosphere is shown in figure 1. On the background of the high intensity of the continuum spectrum some Fraunhoffer absorption doublet lines of sodium and the lines of potassium (from impurities) were detected. Absorption of so far unidentified molecules is also visible. Nearly blackbody radiation revealed that during the combustion the average temperature reached values of 2100 ± 50 K. A similar temperature (about 2200 K) was obtained for the reaction in air and nitrogen gas. Thus, the combustion temperature was greater than the melting point of reactants. It may be also noted that this is in the very range of peak temperatures (2200–2400 K) estimated to occur in solid combustion of the Si–C system [22].

The SHS was carried out with either helium, argon, nitrogen, carbon dioxide, or air as the combustion environment. The initial pressure varied between soft vacuum conditions and 1 MPa. Along with concentrating on optimizing the processing parameters (pressure and reaction environment), the emphasis of this study was also on determining the influence of reactant parameters upon the extent of the reaction and the nature of the products. Thus, the effect of grain size was investigated, too.

A set of combustion syntheses was performed in which the operating parameters (SHS environment, initial pressure and grain size of reactants) were altered. All other variables were kept constant. Tables 1–3 show the results of these parametric studies. All quantitative results

Table 1. Effect of environment gas on combustion synthesis in the Si/PTFE system.

Run no.	Combustion environment	Initial pressure (MPa)	Grain size below (μm)		Peak pressure (MPa)	Product characterization		
			Si	PTFE		Bulk morphology	Unreacted Si content (wt%)	Si conversion (%)
A-1	Vacuum	0.001	43	1	No reaction	—	—	—
A-2	Helium	1.0	43	1	No reaction	—	—	—
A-3	Argon	1.0	43	1	4.0	Soot-like	30.7	32.7
A-4	Nitrogen	1.0	43	1	3.8	Soot-like and sponge-like	32.0	26.4
A-5	Carbon dioxide	1.0	43	1	4.0	Sponge-like	11.9	85.3
A-6	Air	1.0	43	1	3.6	Sponge-like	11.9	84.2

Table 2. Effect of initial pressure on combustion synthesis in the Si/PTFE system.

Run no.	Combustion environment	Initial pressure (MPa)	Grain size below (μm)		Peak pressure (MPa)	Product characterization		
			Si	PTFE		Bulk morphology	Unreacted Si content (wt%)	Si conversion (%)
B-1	Air	0.1	43	1	1.0	Soot-like	26.0	53.0
B-2	Air	0.3	43	1	3.0	Soot-like and sponge-like	18.3	74.6
A-6	Air	1.0	43	1	3.6	sponge-like	11.9	84.2

Table 3. Effect of reactants grain size on combustion synthesis in the Si/PTFE system.

Run no.	Combustion environment	Initial pressure (MPa)	Grain size below (μm)		Peak pressure (MPa)	Product characterization		
			Si	PTFE		Bulk morphology	Unreacted Si content (wt%)	Si conversion (%)
A-6	Air	1.0	43	1	3.6	Sponge-like	11.9	84.2
C-1	Air	1.0	150	1	3.0	Soot-like and sponge-like	23.9	49.7
C-2	Air	1.0	43	100	3.8	Sponge-like	23.5	60.0
C-3	Air	1.0	150	100	2.4	Sponge-like	20.3	71.0

are related to the product collected from the bomb since the crucible material contained residual impurities related to the reaction promoter. The results show that the course of defluorination of PTFE using Si elemental is strongly dependent on the combustion parameters.

No reaction occurred either in vacuum or in helium (table 1), suggesting that the process under consideration is not entirely a typical solid-phase SHS, but depends on the reaction environment, and that some intermediate gas phase radicals [15] are distinctly involved in the formation of the final solid products. In fact, helium gas is known to vigorously quench gas-phase nucleation, e.g., during the synthesis of nanocarbons from carbon gas [22]; this is due to its high thermal conductivity. It is worth noting that in all runs a critical heating of reactants was easily reached regardless of the combustion atmosphere. In the tests carried out either in argon or in nitrogen atmosphere, despite a violently exothermic reaction, only partial transformations of reactants were observed, which is reflected by both the relatively low conversion of starting silicon (about 30%) and the morphology of products (mostly soot-like solids collected in the reactor; see below). Much lower contents of unreacted Si powder

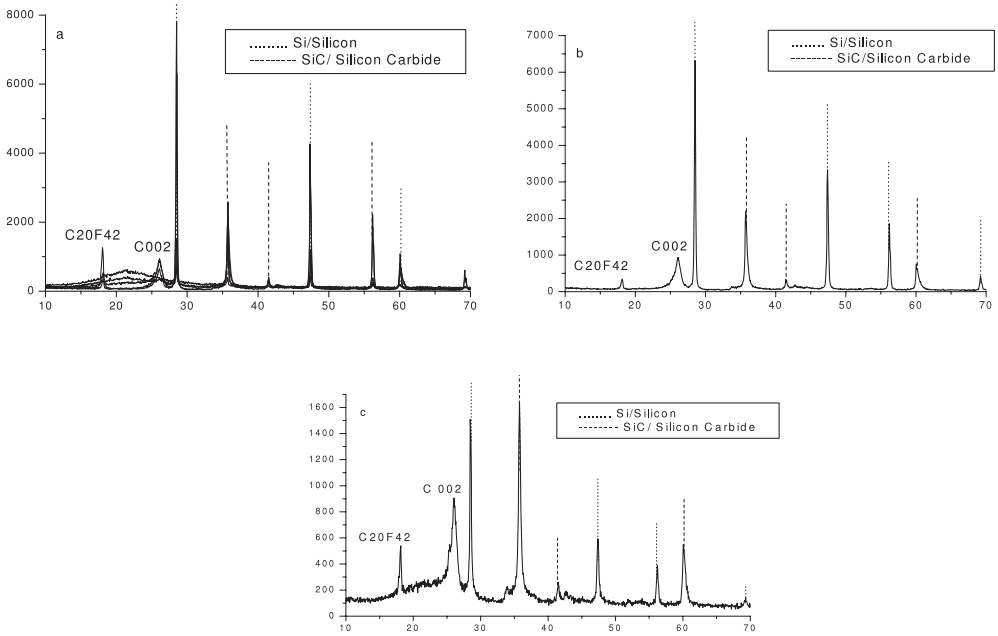

Figure 2. XRD spectra of products resulting from Si/PTFE combustion synthesis: (a) run A-3; (b) run A-4; (c) run A-6.

and hence much higher conversions (between 80–90%) were obtained for runs performed in carbon dioxide and air environments. The sponge-like product, characteristic for fibrous material content [14, 15], almost entirely filled the whole reactor. Surprisingly, the presence of oxygen in the reactor neither shifts the reaction course towards the oxidation of silicon nor the formation of thermodynamically preferable silica, but instead seems rather to favour the formation of fibrous β-SiC, the presence of which in the product, along with some unreacted elemental Si, was confirmed by XRD spectra (figure 2). Thus, the chemical process may be kinetically controlled and a fast quench of reaction products seems to preserve the by-products. Also, oxygen-bearing gaseous intermediates (SiO?) may play an important role in transport/convection phenomena associated with the course of the synthesis. In fact, Rümmeli *et al* [23] noticed that oxygen may play, surprisingly, an important promoting role in the growth of single-walled carbon nanotubes. Yi and Moore [24] also found the SHS formation of NiTi intermetallic compound in air to be dependent on the prior intermediate formation of titanium dioxide, the exothermic nature of which acted as a 'trigger' for the NiTi synthesis.

As shown in table 2, the process yield is not only sensitive to the combustion atmosphere but also distinctly depends on the initial gas pressure. It further confirms that gas-phase processes are clearly involved in the reaction mechanism. With increasing initial air pressure both the extent of reaction and the fibrous character of the collected solids is distinctly enhanced. Higher gas pressure hampers the expansion of reacting radical intermediates, thus increasing the gas phase interaction between them and providing for longer growth duration. At lower pressure this process is otherwise upset by diffusion, cooling and condensation of reaction precursors.

Heat wave propagation velocities can be varied through control of the size of the precursor powder particles, with the larger ones yielding lower velocities. Thus, the set of runs in air with different size of starting reactants was carried out. As shown in table 3, the combustion yield

was essentially independent of the PTFE fractions (1–100 μm), with slightly higher conversion obtained for fine grain size. This indicates that the initial reaction temperature is high enough to initiate the polymer pyrolysis and the formation of gaseous radicals CF$^{\bullet}$. For a fine elemental Si (below 1 μm) the reaction was easily initiated regardless of the initial gas pressure, and high silicon conversions (between 79 and 84%) were obtained. In the case of coarse grain size of starting silicon and PTFE (run C-3) the reaction could only be initiated at the highest pressure applied, while with a fine PTFE (run C-1) the process could be completed even at lower pressure (0.3 MPa). With fine silicon the reaction was completed regardless of the initial air pressure (which was between 0.1 and 1.0 MPa). For both runs with a coarse grain size of elemental Si the content of unreacted silicon in the product was much higher and, consequently, the obtained conversions were lower. Thus, the results show that the most complete combustion occurs in the case of the finest powder mixture. These observations also confirm the involvement of gaseous intermediates in the reaction course which, obviously, are much more efficiently formed in the case of fine reactants.

The results presented in tables 1–3 show that through careful control of process variables, it is possible to obtain high conversion of reactants within very short times. The experiments showed that the highest elemental Si conversions were obtained at initial high pressure in air by using the small grain size of reactants.

In order to further identify the compounds and the structure of the bulk products formed during SHS, x-ray diffraction analysis was performed, and some typical results are summarized in figure 2. It can be seen that all of the recovered solids show a high degree of reaction. Phase identification of as-obtained products was performed by using the XRD patterns, with silicon carbide and unreacted silicon identified as crystalline materials. Also, the presence of some unreacted oxidant ($C_{20}F_{42}$) is observed. The intense silicon carbide peaks can be indexed to the β-SiC lattice structure with stacking faults. Previous bulk-scale Raman studies [12] showed the nanofibres to be comprised of mostly the cubic polytype of SiC. The chemical composition analysis by energy-dispersive x-ray (EDX) spectroscopy and the spacing of the crystallographic planes measured from the high-resolution TEM (HRTEM) images characteristic for β-SiC phase was unambiguously confirmed earlier [15]. Also, the elemental analysis confirmed [15] the chemical purity of the isolated 1D SiC to be at least 98.2 wt%. According to the spectra (figure 2) the highest content of SiC, in relation to unreacted silicon, was found in the run carried out in air (A-6), while the products from runs in Ar and N_2 are quite similar, with lower content of SiC. The quasi-graphite phase (turbostratic graphite) was also found in the products with the strongest peak, (002), at 2θ between 26.5° and 26.65°. From the position of the (002) diffraction peak the spacing of the crystallographic planes can be estimated as between 0.3415 and 0.3422 nm (for HOPG (highly oriented pyrolytic graphite) it is equal to 0.3354 nm).

The morphology of the SHS products is shown by the examples of SEM and TEM images in figures 3–5, respectively. They confirm the conclusions resulting from chemical analyses. Figure 3 presents the images from runs carried out under different atmospheres. Only a few nanofibres could be found in products from runs in argon (3(a)) and nitrogen (3(b)) while a much higher content was observed from runs in carbon dioxide 3 (c) and air 3 (d). The product from combustion under low pressure (figure 4(a)) contains very few nanofibres while with increasing pressure its amount distinctly increases (figures 4(b) and 3(d)—1 MPa). A large grain size of starting silicon (150 μm—figures 4(c) and (h)) results generally in a lower content of nanofibres, while the effect of PTFE is not so pronounced (4(f)). The crucible residue (4(d)) usually contains fewer nanofibres with some 3D SiC nanocrystallites observed (4(e)). This confirms that the chemical transformation of reactants is commenced in the crucible, with the main course of gas-phase reaction being outside in the reactor. The highest content of SiC nanofibres was found in the sample collected from the reactor's wall, which points to the

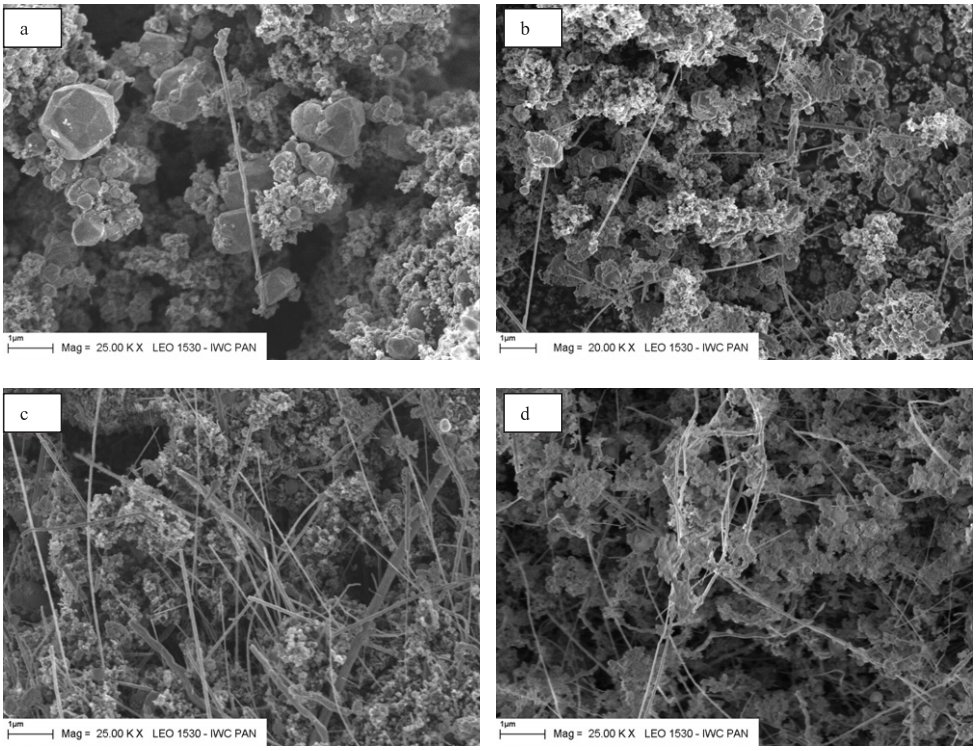

Figure 3. SEM images: (a) run A-3; (b) run A-4; (c) run A-5; (d) run A-6.

importance of fast quench of products. 1D SiC nanofibres typically have diameters ranging from several to several tens of nanometres, lengths up to several tens of microns and aspect ratio well above 10^3. As one can see, they were present in almost all samples; however, they had different concentrations. The 1D nanostructures are usually linked together in a spaghetti-like manner. The yield of nanofibres is significantly higher for runs carried out under oxygen presence and at higher pressure.

TEM examinations (figure 5) revealed further detailed structural features of the SHS products which contain (figure 5(a)) mostly SiC (EDX analysis) nanofibres along with unreacted silicon and carbon material. The latter forms mostly onion-like, relatively well crystallized nanostructures (20–80 nm in diameter) built of several graphene layers (figure 5(b)). The interlayer distance between graphene planes was measured to be about 0.332 nm. The nanofibres exhibit similar structural characteristics, namely, they are well-crystallized, elongated single crystals of 1D SiC (from a few to several tens of nanometres in diameter); see figure 5(c). They have primarily smooth and straight whisker-like morphology, with some of them possessing bends and kinks. The compartment-like morphology may suggest sequential growth. The liquid globules found on the tip of some nanofibres could suggest a vapour–liquid–solid (VLS) growth mechanism [25]. The spacing of the crystallographic planes (HRTEM images; see figure 5(d)) is about 0.225 nm, which is consistent with the (111) lattice planes of crystalline β-SiC. The centre nanofibre is wrapped in a relatively uniform, outer layer of SiO_2 (EDX analysis), a few nanometres thick.

Depending on the process parameters, the total carbon content (from the elemental analyses) of the solid products exceeded 80 wt%. Calcination of the sample resulted in a distinct

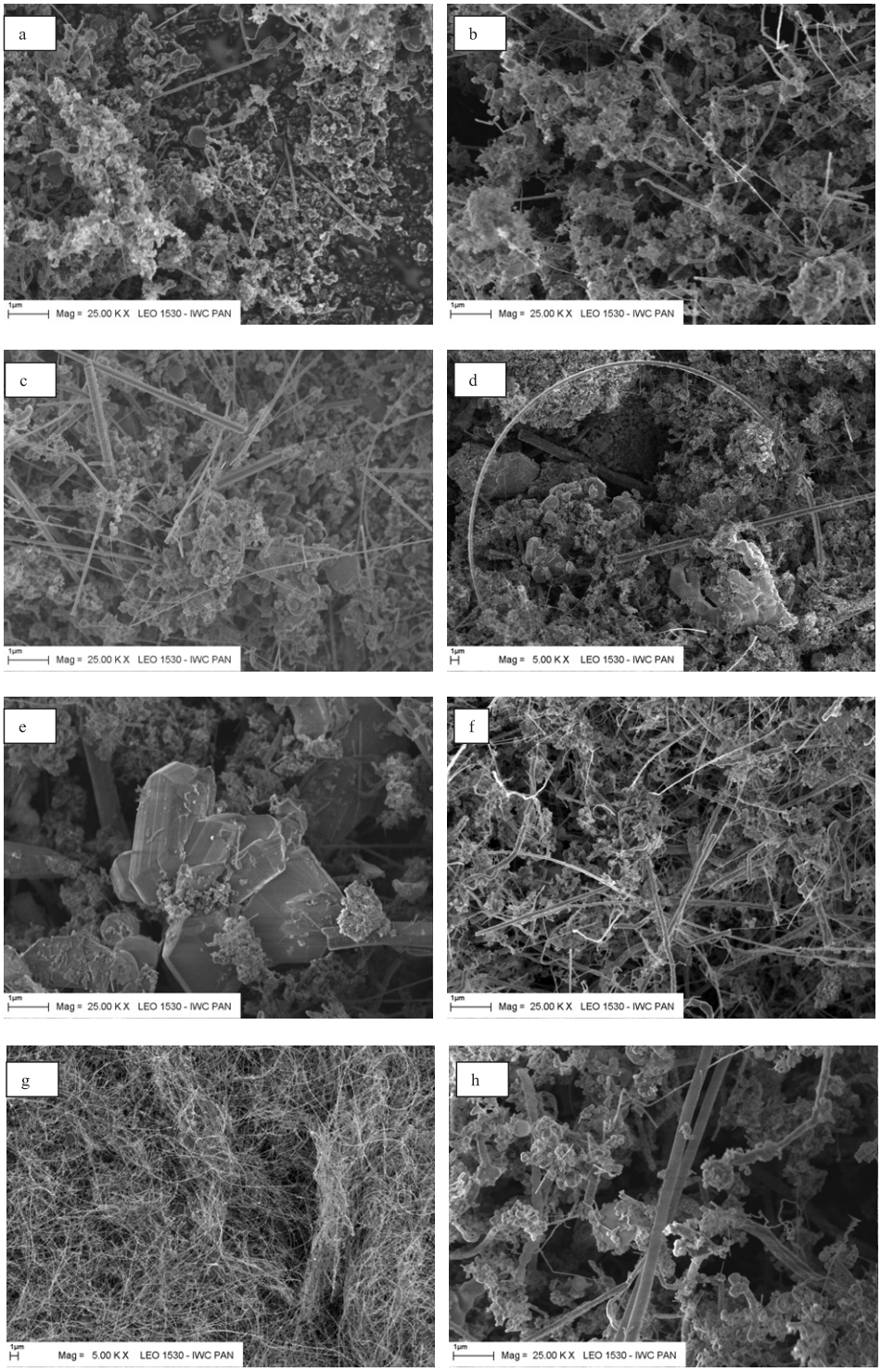

Figure 4. SEM images: (a) run B-1; (b) run B-2; (c) run C-1; (d) and (e) run C-2, sample from crucible; (f) run C-2, sample averaged from reactor; (g) run C-2; sample from reactor's wall; (h) run C-3.

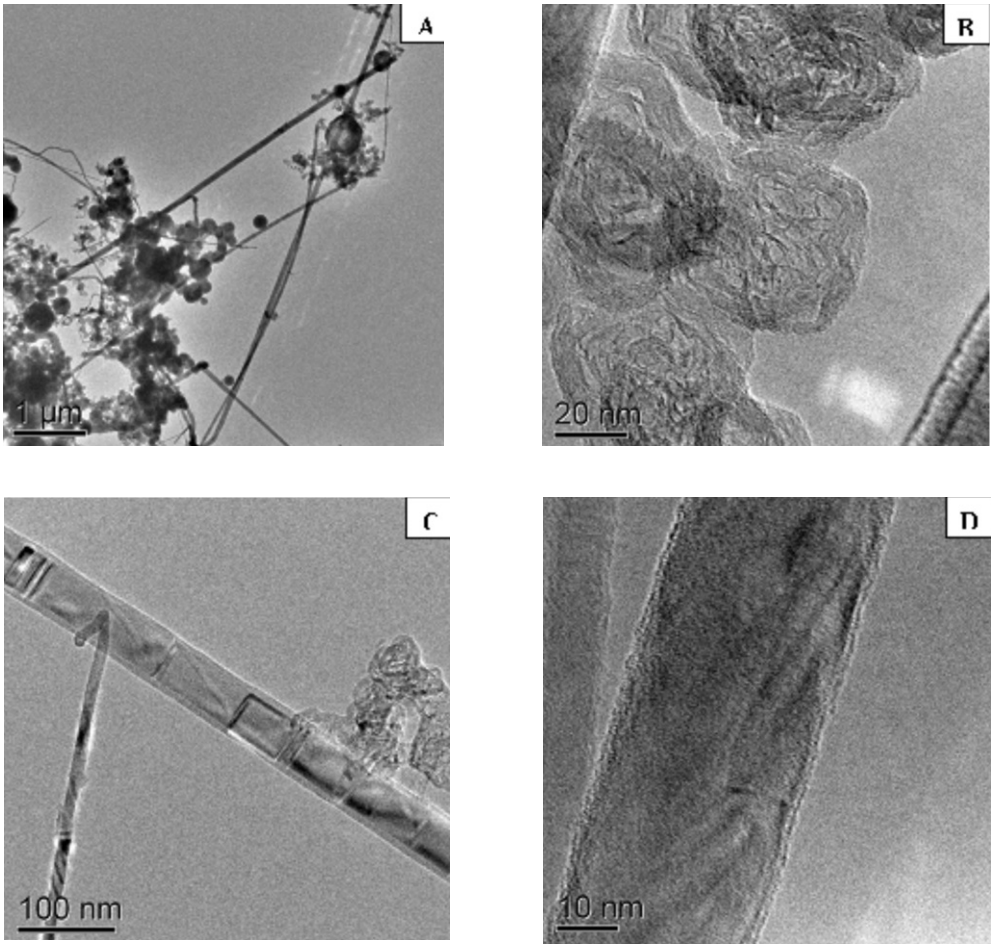

Figure 5. TEM/HRTEM images of products (run A-6).

decrease of carbon content (up to 70%) due to the oxidation and removal of amorphous carbon. The residual carbon (about 26 wt%) can be related to carbide phases due to its resistance against oxidation at the heating temperature. Thus, the chemical purity of the obtained 1D SiC could be estimated to be about 90 wt%, which is in close agreement with the result of a silicon carbide purification and isolation protocol (by using wet chemistry [15]) yielding 98% purity.

4. Conclusions

In summary, we have completed a detailed parametric investigation of 1D SiC nanomaterial fabrication by SHS from mixed elemental Si and PTFE. This self-induced growth process can yield β-SiC nanofibres about 20–100 nm in diameter with lengths of several microns. The nucleation mechanism involving radical gaseous species, with evident involvement of oxygen-containing intermediates, is responsible for 1D nanostructure growth. A conversion of starting elemental Si of above 90% was achieved while the purification of products yielded SiC nanofibres at least 90% pure. Therefore, we believe that this approach may open up a new field for prosperous applications of SiC nanomaterials.

Acknowledgments

This work was supported by the Ministry of Science and Higher Education through the Department of Chemistry, Warsaw University, under Grant No. 3 T08D 012 28. We also acknowledge M Rümmeli and T Gemming from IFW Dresden, Germany, for their assistance in the TEM measurements. M Bystrzejewski thanks the Foundation for Polish Science (FNP) for financial support.

References

[1] Munir Z A and Holt J B 1990 *Combustion and Plasma Synthesis of High Temperature Materials* (New York: VCH)
[2] Crider J F 1982 *Ceram. Eng. Sci. Proc.* **3** 519
[3] Munir Z A 1988 *Ceram. Bull.* **67** 342
[4] Aruna S T and Rajam K S 2004 *Mater. Res. Bull.* **39** 157
[5] Wu K H, Huang W C, Yang C C and Hsu J S 2005 *Mater. Res. Bull.* **40** 239
[6] Cano I G and Rodriguez M A 2004 *Sci. Mater.* **50** 383
[7] Takacs L 2002 *Prog. Mater. Sci.* **47** 355
[8] Patil K C 1993 *Bull. Mater. Sci.* **16** 533
[9] Zenotchkine M, Shuba R and Chen I W 2004 *J. Am. Ceram. Soc.* **87** 1040
[10] Dali S E and Chockalongam M J 2001 *Mater. Chem. Phys.* **70** 73
[11] Toniolo J C, Lima M D, Takimi A S and Bergmann C P 2005 *Mater. Res. Bull.* **40** 561
[12] Jiang J, Wang P, He W, Chen W, Zhuang H, Cheng Y and Yan D 2004 *J. Am. Ceram. Soc.* **87** 703
[13] Howard J B, McKinnon J T, Makarovsky Y, Laufler A L and Johnson M E 1991 *Nature* **352** 139
[14] Huczko A, Lange H, Chojecki G, Cudziło S, Zhu Y Q, Kroto H W and Walton D R M 2003 *J. Phys. Chem.* B **107** 2519
[15] Huczko A, Bystrzejewski M, Lange H, Fabianowska A, Cudziło S, Panas A and Szala M 2005 *J. Phys. Chem.* B **109** 16244
[16] Cudziło S, Bystrzejewski M, Lange H and Huczko A 2005 *Carbon* **43** 1778
[17] Huczko A, Lange H, Bystrzejewski M, Fabianowska A, Cudziło S, Szala M, Katan A, Patil A V, Heeres E C and T H Oosterkamp 2006 *XXII IWEPNM (Kirchberg Austria, March 2006)* p 56 (Abstract Book)
[18] Huczko A, Lange H, Bystrzejewski M, Rutkowska A, Cudziło S, Szala M and Wee A T S 2006 *Phys. Status Solidi* b **243** 3297
[19] Cambaz Z G, Yushin G N, Gogotsi Y, Vyshnyakova K L and Pereselentseva L N 2006 *J. Am. Ceram. Soc.* **89** 509
[20] Han W, Fan S, Li Q, Liang W, Gu B and Yu D 1997 *Chem. Phys. Lett.* **256** 374
[21] Ye H, Titchenal N, Gogotsi Y and Ko F 2005 *Adv. Mater.* **17** 1531
[22] Taylor R 1999 *Lecture Notes on Fullerene Chemistry* (London: Imperial College Press)
[23] Rümmeli M H, Borowiak-Palen E and Gemming T 2005 *Nano Lett.* **5** 1209
[24] Yi H and Moore J J 1989 *J. Mater. Sci.* **24** 3456
[25] Wagner R S and Ellis W C 1964 *Appl. Phys. Lett.* **4** 89